

Theoretical Calculations of Pressure Broadening Coefficients  
for H<sub>2</sub>O Perturbed by H ydrogen or Helium Gas

Robert R. Gamache† and Richard Lynch††  
University of Massachusetts Lowell  
Center for Atmospheric Research  
450 Aiken Street  
Lowell, MA, 01854

and

Linda R. Brown  
Jet Propulsion laboratory  
California Institute of Technology  
4800 Oak Grove Dr.  
Pasadena, CA 91109

Pages        20  
Tables       7  
Figures      5

† All correspondence should be sent to

Prof. Robert R. Gamache

University of Massachusetts Lowell

Center for Atmospheric Research

450 Aiken Street

Lowell, MA, 01854 USA

†† Current address

Wentworth Institute of '1'ethnology

550 Huntington Ave.

Boston, MA 02135

## AIMTRACT

To aid in the reduction of remote-sensing data from the outer planets, collision-broadened half widths are calculated for water vapor broadened by  $\text{H}_2$  and are estimated for He-broadening. The model used is a fully complex implementation of the Robert and Bonamy formalism with parabolic trajectories and all relevant terms in the interaction potential. Calculations are performed for 386 pure rotational transitions of  $\text{H}_2\text{O}$  with  $J''=0$  to 14 and  $Ka''=0$  to 8. In addition, the temperature dependence of the half width is computed for a temperature range from 200 to 750 K for thirty-three transitions with  $J''=1$  to 10 and  $Ka''=0$  to 8. The calculations are compared with known measurements of pure rotational and  $v_2$  lines and good agreement is observed (-2 and -4 percent difference respectively). Finally, methods for estimating half widths for  $\text{H}_2$ - and He-broadening are presented.

## INTRODUCTION

The atmospheres of the giant planets are made mostly of  $H_2$  and He, the same constituents that are the dominant constituents of the Sun. This composition reflects the ability of the massive giant planets to have gravitationally captured large amounts of gases from their birthplace in the primordial solar nebula as well as solids (e. g., water) that were eventually volatilized into heavier gases in their atmospheres. In contrast, the terrestrial planets, such as Earth and Venus, contain atmospheric gases derived almost exclusively from the solid component of the solar nebula. By obtaining accurate estimates of the water abundance in the atmospheres of the giant planets, we will be able to place important constraints on the relative efficiency with which they accumulated gases and solids from the primordial solar nebula.

There are selected regions of the thermal infrared spectrum of the giant planets, especially Jupiter, that are known to contain water vapor features. One example is a portion of the so-called 5 micron "window". However, when viewed from space, much of the emission comes from altitude regions that are cold enough for water to follow approximately its saturation vapor pressure curve and what is needed is its abundance in the hotter, well mixed region below the water clouds. The Net flux radiometer experiment (NFR) on the Galileo probe contained several broad band channels that encompass water features to obtain data below the water condensation region. Such measurements were made during the descent of the Galileo probe in early December, 1995.

In order to retrieve accurate estimates of water mixing ratio from these data, it is essential that all spectroscopic parameters of the relevant water lines be well known. The data for the molecular absorption parameters are that of Rothman *et al*. The molecular absorption data for each spectral transition (line) consist of at least the resonant frequency, line intensity, air-broadened halfwidth, and lower state energy. In addition HITRAN<sup>1</sup> also contains the temperature dependence of the air-broadened halfwidth, weighted transition moment squared, self-broadened half width, line shift, quantum identification of the transition and some error and reference codes. While the line strengths and energy levels are relatively well known, the pressure broadening halfwidths have major uncertainties in them (at least a factor of several) that would limit water abundance determinations severely. For the atmospheres of giant planets, such as Jupiter, the broadening by H<sub>2</sub> and He must be known. Until recently, there was a gross uncertainty about even room-temperature H<sub>2</sub> - broadened half widths, and a similar situation exists for water broadening by He, although estimates are acceptable here because H<sub>2</sub> broadening dominates. The temperatures of interest are centered around room temperature and range from 200 K to 400 K. The pressures of interest are centered around 5-10 bars and range from 1 to 20 bars.<sup>2-4</sup> Since one is dealing with large optical paths, even weak optical transitions must be accounted for. Hence, a database of half widths for J and Ka quantum numbers up to 20 and 15, respectively, should be made available.

The effect of errors in the halfwidth on retrieved profiles has been systematically investigated<sup>5-7</sup> with the conclusion that inaccurate collision-broadened halfwidth values lead to significant errors in retrieved profiles,

Hydrogen-broadened half widths of water vapor have been measured for some 640 transitions.<sup>8-12</sup> Two of these<sup>8,9</sup> are room temperature values for the 22 GHz line while the 183 and 380 GHz lines are observed at different temperatures by Dutta et al.<sup>10</sup> Recently Langlois et al.<sup>11</sup> have made 11 diode laser measurements at different temperatures in the 1.4  $\mu$  m region and Brown and Plymate<sup>12</sup> have reported 630 room-temperature widths in the pure rotational, and three fundamental bands between 55 and 4045  $\text{cm}^{-1}$ . To our knowledge, there have been no theoretical calculations. For He-broadening only 11 lines have been measured<sup>9,10,13-16</sup> and the temperature dependence has been considered for some of the lines. These latter data are insufficient to validate a theoretical calculation, but they allow the He-broadening of water to be estimated by taking the ratio of He-broadened half widths and half widths for other broadening species such as  $\text{N}_2$ ,  $\text{O}_2$ ,  $\text{H}_2$ , or  $\text{CO}_2$ .

In this work Hz-broadened  $\text{H}_2\text{O}$  halfwidths are calculated using a fully complex implementation of the theory of Robert and Bonamy<sup>17</sup> (FCRB).<sup>18</sup> For the Galileo probe experiments, the two dominant water bands are the pure rotational and  $\nu_2$  fundamental. Although the Watson constants are known for both bands<sup>19</sup> the initial calculations of the wavefunctions and energies for the states consider the ground vibration state only. The work of Brown and Plymate<sup>12</sup> and the survey of Gamache et al.<sup>20</sup> both indicate that the maximum error introduced by this approximation should be less than 5%. Calculations of half width are performed for the lower state rotational quantum numbers,  $J''$  and  $K_a''$ , varying from 0 to 14 and 0 to 8, respectively. The temperature dependence of the half widths is studied over a range from 200-750 K (the

extended temperature range is to test the theoretical model). The results of these calculations are compared with the experimental values.

Different methods to estimate the halfwidths for transitions not considered in this study are investigated. Finally, we determine a method for estimating halfwidth values for He-broadening of water vapor using the measured or calculated values for other perturbing species. While there are limitations on such a method, it does allow a guess at the He-broadened values which may not be as critical due to the lesser amount of this gas in the atmospheres of the planets,

## THEORETICAL CALCULATIONS

The theoretical calculations made here are based on a fully complex implementation of the theory of Robert-Bonamy<sup>17</sup> (FCRB) applied to asymmetric rotor molecules.<sup>21-23</sup> The atom-atom coefficients are corrected<sup>24</sup> to explain some inconsistencies in previous calculations.<sup>25</sup> The formalism presented here is slightly different from Ref. 24 in that a more manageable expression is employed for the atom-atom potential allowing more complete expansions to be considered. A major difficulty in the RB method is evaluating the Fourier-laplace transforms of correlation functions, which arise in the theory because of the semiclassical treatment of translational motion. Computer-assisted algebraic methods have proved very useful in addressing this. Emphasis throughout is placed on generality, insofar as the formulas are complex-valued (yielding line shifts as well as halfwidths) and for the most part suitable for any pair of colliding molecules.

The intermolecular potential appears in the theory as a spherical tensor expansion in the intermolecular separation  $R$ ,

$$V^{(\text{R-frame})}(\mathbf{t}) = \sum_{\substack{\vec{l}m \\ \vec{m}q}} v_{\vec{l}m \vec{m}q} \frac{D_{m m_1}^{l_1}(\Omega_1) D_{-m-m_2}^{l_2}(\Omega_2)}{R^q} \quad (1)$$

The  $D$ 's are components of spherical tensors (Wigner rotation matrices<sup>26</sup>) as given by Gray and Gubbins.<sup>27</sup> Symbols  $\Omega_1$  and  $\Omega_2$  specify the orientation of the molecule-fixed frame within the conventional "R-frame".<sup>28</sup> Coefficients  $v_{\vec{l}m \vec{m}q}$  depend on how the molecules are situated within the molecule-fixed frame. In the present calculations, water vapor is taken in the  $\text{IR}$  representation<sup>29</sup> and  $\text{N}_2$  lies along the  $z$ -axis.

The radial parts of Eq. (1) are not the most general form, but suffice to describe both electrostatic and atom-atom Lennard-Jones 6-12 interactions. The electrostatic potential is given by an expansion<sup>27,28</sup> of the charge distribution in terms of the electric moments of the molecules, e.g. dipole-dipole, dipole-quadrupole, etc.

$$V_{1,2}^{\text{elec}} = V_{\mu_1\mu_2} + V_{\mu_1\theta_2} + V_{\theta_1\mu_2} + V_{\theta_1\theta_2} + V_{\theta_1\theta_2} + \dots \quad (2)$$

Here the contributing terms are the dipole( $\text{H}_2\text{O}$ )-quadrupole( $\text{H}_2$ ) and quadrupole( $\text{H}_2\text{O}$ )-quadrupole( $\text{H}_2$ ) interactions. The values of the dipole and quadrupole moment components of  $\text{H}_2\text{O}$  are taken from Refs. 30 and 31 respectively, and the quadrupole moment of  $\text{H}_2$  is taken from Ref. 32. In the derivation of atom-atom coefficients, it is convenient to define an order  $Q$  of the atom-atom expansion as,  $Q=(q-q_0)$ , with  $q_0$  typically 6 or 12. In previous formulations, expressions for anisotropic atom-atom coefficients  $v_{\vec{l}m \vec{m}q}$  have been obtained explicitly to order  $Q=4$ , using for example the algebraic method of Labani et al.<sup>21-23</sup> To consider higher

orders the method of Refs. 21-23 are cumbersome, even with computer assistance.<sup>24</sup> Therefore we use the expressions derived by Sack<sup>33</sup> and Downs et al.<sup>34</sup> (see also Gray and Gubbins<sup>27</sup>) to determine the coefficients of the atom-atom potential. (For example see Appendix A of Ref. 35) A static, zero-rank expansion of the atom-atom potential ( $l_1$  and  $l_2$  both zero) defines the isotropic potential used to compute the translational motion of the molecules.

The expression for the halfwidth at half height and the line shift in RB theory is

$$\phi_{if} = (\gamma_{if} - i\delta_{if}) = \frac{n_2}{2\pi c p} \sum P_2 \int_0^\infty v f(v) dv \int_0^\infty 2\pi b (1 - C - S'') db \quad (3)$$

where  $v$  is the relative velocity of the two molecules,  $b$  the impact parameter,  $n_2$  the number density of the perturber gas at pressure  $p$ . The observed half width is assumed to be a linear function of pressure,  $\phi_{if}^{obs} = p\phi_{if}$ . We assume the mean relative thermal velocity approximation, replacing the Maxwell-Boltzmann distribution  $f(v)$  by  $\delta(v - \bar{v})$ , where  $\bar{v}$  is the average relative velocity. The interruption function,  $S_{if}$ , is given by

$$S_{if} = S_{1,i}^* + S_{1,f} + S_{2,i2}^* + S_{2,f2} + S_{2,middle} \quad (4)$$

The components are complex-valued analogs of terms familiar from ATC<sup>36-37</sup> theory. The  $S_1$  terms are developed in Ref. 18. Both "outer" terms  $S_{2,i2}$  and  $S_{2,f2}$  and "middle" term  $S_{2,f2i2}$  are expressed in terms of resonance functions  $F$  and reduced Liouville matrix elements  $D$ ,

$$S_{2,i2} = \frac{1}{\hbar^2 [J_i] [J_2]} \sum_{i', 2'} \sum_{\overrightarrow{lm^a m^b}} D_{ii'} \overrightarrow{lm^a m^b} F_{\overrightarrow{lm^a m^b}}(\omega) \quad (5)$$

$$S_{2,f2i2} = \frac{-2}{\hbar^2 [J_2]} \sum_{2'} \sum_{\overrightarrow{lm^a m^b}} D_{if,if'} \overrightarrow{lm^a m^b} F_{\overrightarrow{lm^a m^b}}(\omega) (-)^{J_i + J_f + l_i} \begin{Bmatrix} J_i & J_i & l_i \\ J_f & J_f & J \end{Bmatrix} \quad (6)$$

where  $S_{2,f2}$  is obtained from Eq. 5 by the substitutions  $i \rightarrow f$  and  $i' \rightarrow f'$ . We use the notation  $[J] \equiv 2J + 1$ ,

The exponential form of Eq. (3) comes about as a result of a cumulant formulation of the perturbation expansion for the collision.<sup>38</sup> Because of it, imaginary parts of  $S$  affect not only the shift, but the width as well, an effect not achieved in ATC theory.

As stated above, some difficulty arises in the evaluation of the integrals over translational degrees of freedom because of the large orders and tensorial ranks required. This is discussed in Ref. 35. Techniques for evaluating the fully complex integrals in the parabolic approximation are described elsewhere.<sup>18,39</sup>

## RESULTS and DISCUSSION

All molecular 'constants used in the calculations are the best available from the literature. Values of electrostatic moments for  $H_2O$  and  $H_2$  are given in Table 1. The atom-atom potential employed in this work is an expansion to 4<sup>th</sup> order with  $l_1$  and  $l_2$  having maximum values of 2. The Lennard-Jones parameters necessary for the atom-atom component of the potential can be determined by fitting virial data<sup>40</sup> or by using combination rules.<sup>28</sup> Because of a lack of virial data for the  $H_2O-H_2$  system,

combination rules were used to obtain hetero-atomic Lennard-Jones parameters ( $\epsilon_{HO}, \sigma_{HO}$ ) from homo-atomic ones quoted by Bouanich<sup>40</sup> ( $\epsilon_{HH}, \sigma_{HH}$ , etc.), with results given in Table II. The isotropic Lennard-Jones parameters  $\epsilon_{iso}$  and  $\sigma_{iso}$ , are derived from these atom-atom parameters by formal expansion. No attempt is made to optimize the molecular constants to improve the match with experimental line widths, although such adjustments would certainly be justified considering the probable uncertainties of some of the constants.

All transitions for  $\text{H}_2^{16}\text{O}$  in the region 1500-2500  $\text{cm}^{-1}$  for which the intensity is greater than  $1 \times 10^{-23} \text{ cm}^{-1}/\text{molecule cm}^2$  and  $J''$  is less than 15 are selected from the HITRAN database. The cutoff at  $J''$  less than 15 is necessary due to the current limitations of the computer resources to address this problem. Because the calculations neglect the vibrational dependence, only lines with unique sets of rotational quantum numbers are retained using the assumption that the widths are the same for the pairs of transitions with upper and lower quantum numbers interchanged. The resulting calculated half widths in units of  $\text{cm}^{-1}/\text{atm}$  at 296 K are given in Table 111.

Additional calculations at other temperatures are made to allow direct comparison with the available measurements. In Table 111, the calculated half widths are compared with the pure-rotation and  $\nu_2$  band measurements of Brown and Plymate.<sup>12</sup> The columns in the table are the upper and lower state rotational quantum numbers, the calculated half width at 296 K in  $\text{cm}^{-1}/\text{atm}$ , and the next 4 columns are measured values with the percent uncertainty in parentheses and the percent difference,  $(\text{Exp}-\text{Cal})/\text{Exp}$ , for the pure rotational and  $\nu_2$  bands,

respectively. In Table IV, the calculations of the 22 GHz line (616←523) of water vapor at 293 and 300 K and the 183 and 380 GHz lines at 300 K, (313←220) and (414←321) respectively are compared with the measurements of Liebe and Dillon<sup>8</sup> and Kasuga et al.,<sup>9</sup> and Dutta et al.<sup>10</sup>

Brown and Plymate<sup>12</sup> have made measurements for 64 pure rotation and 273  $\nu_2$  transitions of  $H_2O$  broadened by  $H_2$  at 295 K with a precision of 2 to 7%. Because the calculations made here are for the ground state only the pairs of lines with the rotational quantum numbers exchanged in the experimental data are averaged together (i.e.  $f \leftarrow i$  and  $i \leftarrow f$ ). This reduces the number of  $\nu_2$  transitions to compare with to 161. These experimental results are listed in Table 111 with the calculations. For the transitions considered, the half widths vary by factors of 3 or 4 from low J, K to high J, low K. A comparison of the calculated values with those of Brown and Plymate is given in Fig. 1 where the percent difference is plotted versus an energy ( $E''$ ) ordered index  $\{J''(J''+1)+Ka''-Kc''+1\}$ . Note, because of the small temperature difference (1 °K) no temperature correction is applied to the data. For the pure rotation data the average percent difference between the calculated and measured values is -1.9%, the average absolute percent difference is 3.8, and the maximum and minimum deviations are about 10%. Comparison with the  $\nu_2$  data shows a -3.8 percent difference with 21 of the 161 points showing differences between 10 and 20%. Since these values are obtained from only single, transitions rather than averaged pairs, it is difficult to assess if this is due to experimental errors or real vibration] effects. Also evident is that the calculated values are greater than the measurements for  $J'' < 8$  but for  $J'' > 8$  this appears to be reversed, however there are limited experimental data.

A comparison of the FCRB calculation with the other pure rotational measurements<sup>8-10</sup> is shown in Table IV. The calculations for the 183 and 380 GHz transitions are within -6.0 and 2.6% of the measurements reported by Dutta et al.<sup>10</sup> For the two studies of the 22 GHz line,<sup>8,9</sup> the calculation is in better agreement with the Kasuga et al.<sup>9</sup> value despite it having a much larger error bar.

Thirty-three transitions from  $J''=1$  to 10 and  $K_a''=0$  to 8 are chosen to study the structure of the temperature dependence of the half width as a function of  $J''$  and  $K_a''$  and to compare with the experimental measurements of Langlois et al.<sup>11</sup> and Dutta et al.<sup>10</sup> Calculations of the halfwidth are made at the temperatures 200, 250, 296, 400, and 750 K. The temperature dependence of the half width is taken as<sup>41</sup>

$$\gamma(T) = \gamma(T_0) \left( \frac{T_0}{T} \right)^n, \quad (7)$$

where the reference value ( $T_0$ ) was taken at 296K. The calculated half widths at the temperatures studied are fit to Eq. (7) to give the temperature exponent,  $n$ , and the correlation coefficient of the fit. Figure 2 shows the results of the fit for the minimum and maximum temperature exponents determined in this work.

In Table V, the temperature exponents,  $n$ , determined in this study are presented with an estimated uncertainty and the data from Dutta et al.<sup>10</sup> and Langlois et al.<sup>11</sup> The  $H_2O-H_2$  measurements of Dutta et al. show large deviations from the simple power law (Eq. (7)) at low temperature (100 K). The results from this work (see Fig. 2) demonstrate the same general feature for some of the transitions. To account for these features, an uncertainty is determined for each transition by the following

procedure. Values of  $n$  are determined using any two of the five calculated points. This generates nine 2-point values of  $n$ . The uncertainty assigned to the calculation is the maximum difference between the least-squares fit value and the nine 2-point values. Figure 3 displays the temperature exponent data from this work and that of Refs. 10 and 11. For the 13 experimental measurements, 6 of the calculated temperature exponents are within the experimental error limits, 4 others are close, and 3 show large differences. An unexplained feature of the data of Ref. 11 is the discrepancy between the measured  $n$  values for pairs of lines;  $3\ 3\ 0 \leftarrow 3\ 3\ 1$  and  $3\ 3\ 1 \leftarrow 3\ 3\ 0$ , and  $4\ 3\ 2 \leftarrow 4\ 3\ 1$  and  $4\ 3\ 1 \leftarrow 4\ 3\ 2$  (lines 10 and 11, and 14 and 15, respectively in Table V and Fig. 3). Neglecting vibrational dependence, which should be small, theory states that the value of  $n$  should be the same for these pairs. The experiments] values however are (0.35, 0.76,) and (0.39, 0.26) for the pairs, respectively.

Figure 4 shows the temperature exponent versus  $K_a''-K_c''$  for transitions studied with  $J''=5$ . The temperature exponents are transition dependent and range roughly from 0.19 to 0.71. Figures. 3 and 4 demonstrate the difficulty to predict the temperature exponent of a particular transition based on the values from other transitions. This may be significant since Chu et al.<sup>7</sup> have shown that a change of the temperature exponents from 0.5 to 0.7 can introduce 5% error to retrieved mixing ratios at some altitudes.

#### ESTIMATED HALF-WIDTHS of H<sub>2</sub>- and He-BROADENED WATER

The half widths of some 386 transitions of water vapor are calculated in this work. For application to planetary radiative transfer studies all the

lines of significant absorption within the spectral range must be known. Currently the HITRAN database lists 1763 transitions for the  $\nu_2$  band. The lines for which we make calculations contain about 80% of the intensity of the  $\nu_2$  band. Hence there is a need to approximate the half widths for the transitions for which there are no data. These will be mostly transitions with  $J'' > 14$  and  $\Delta K > 3$  (see Table 111).

Because previous works only provided the  $H_2$ -broadened half widths for a limited number of transitions (stronger lines up to  $J=12$ ) of water vapor, all other transitions could only be guessed at. This can be done<sup>42,43</sup> by scaling values derived for some other perturbing species such as  $N_2$  or air. Such procedures yield approximate values for transitions where the half widths for another perturbing species are known. Often default values must be used. Better estimates of the half width are provided by the procedures described below.

Two different methods for estimating halfwidths are considered. First, a simple average of the half width as a function of  $(J'' + J')/2$  is made. Second, a polynomial in  $J''$  and  $Ka''$  is used to fit the calculated halfwidths. Here, the polynomial expression employed by Gamache et al.<sup>44</sup> is used,

$$\gamma(\text{poly}) = b_0 - b_1 \left( \frac{J'' + J'}{2} \right) + b_2 \left( \frac{J'' + J'}{2} \right)^2 + b_3 \left( \frac{Ka'' + Ka'}{2} \right). \quad (8)$$

The coefficients (and their standard deviations in parenthesis) are obtained by least-squares fitting to the calculated data yielding  $b_0 = 0.09312/1$  (0.002),  $b_1 = -0.7192 \times 10^{-2}$  ( $0.6 \times 10^{-3}$ ),  $b_2 = 0.2451 \times 10^{-3}$  ( $0.4 \times 10^{-4}$ ), and  $b_3 = 0.43104 \times 10^{-4}$  ( $0.2 \times 10^{-3}$ ).

The halfwidths from the averaging procedure and from the polynomial were compared with the calculated results. The average

percent difference (API>), the average absolute percent difference (AAPD), and the minimum and maximum percent differences were calculated as a function of  $(J''+J')/2$ . The AAPD for all the lines studied is 11%) for both methods and the maximum and minimum percent differences are 23 and -50% for the averaging method and 25 and -56% for the polynomial method. In Fig. 5 the percent difference versus  $(J''+J)/2$  is plotted for the averaging method (dots) and the polynomial method (+ symbol). Note the polynomial results are shifted on the  $(J'' - J)/2$  axis in order to better compare the methods. The figure gives an estimation of the range of error one might expect when using the methods to predict halfwidths that are unknown. Because the polynomial results are limited to only the fit range, have a slightly higher uncertainty, and for speed of calculation, the averaging method is recommended for determining half widths not listed in Table III. It should be realized, however, that the estimated values have large uncertainties.

in Table VI the measured values of the He-broadened half width of water vapor are presented. When available the temperature coefficient is also given. With this data the ratios to half widths for other perturbing species can be formed which will allow an estimate of the He-broadened values. Because of the large uncertainties and the temperature of the study of Ref. 16 (the last seven entries in the table.) these data are not considered in the analysis. Table VII gives the three remaining transitions for He-broadened data and the corresponding half width and ratio with other broadening species. The experimental data of Table VI has been corrected to 296 K using the temperature exponents listed in the table. The rotational state quantum numbers labeled 1, 2, and 3 in Table VII correspond to the transitions  $3 \leftarrow 2$ ,  $4 \leftarrow 3$ , and  $6 \leftarrow 5$ .

respectively. All ratios are the He-broadened value divided by the value for the particular perturbing species and all half widths are in units of  $\text{cm}^{-1}/\text{atm}$  at 296 K. The other values in the table are calculated values from Ref. 45 for  $\text{N}_2$ - and  $\text{O}_2$ -broadening, from Ref.44 for  $\text{CO}_2$ - broadening, and from this work for Hz-broadening. The ratios show roughly a 30% variation. Given this and the few lines considered a minimum uncertainty of 50% might be assigned in the scaled He-broadened values,

## SUMMARY

A database of Hz-broadened halfwidths of water vapor is calculated for 386 pure rotational perpendicular transitions of water for  $J''$  up to 14 and  $Ka''$  up to 8 using the fully complex Robert-Bonamy formalism. These values are found to reproduce both the available pure rotational and  $\nu_2$  measurements to within 6% or better for the most part. Comparison with the recent measurements of Brown and Plymate shows better than 2% agreement on average for the pure rotation band (68 transitions) and better than 4% for the  $\nu_2$  band (161 transitions). The temperature dependence of the halfwidth is calculated for 33 transitions from  $J''=1$  to 10. The results show a large spread in the values of the temperature exponents and no systematic trends with the quantum numbers of transitions involved. Methods to estimate the Hz-broadened half widths are presented but caution should be used when applying them due to the high uncertainty. A method is also presented to estimate the He-broadened half widths of  $\text{H}_2\text{O}$ . The resulting halfwidths have high uncertainty, however because of the lesser amount of this gas in the atmospheres of the planets these estimated half widths are useful. Calculations are currently

underway to explore the molecular constants for the atom-atom potential and the vibrational dependence of the measured halfwidths presented in Ref. 12.

## ACKNOWLEDGMENT

The authors would like to dedicate this work to the late Dr. Jim Pollack and acknowledge the many helpful discussions with him on the problem of H<sub>2</sub> - and He-broadening of water vapor. Funds for the support of this study have been allocated by the NASA-Ames Research Center, Moffett Field, California, under Interchange No. NCC2-5029 and by the National Science Foundation through Grant No. ATM-94] 5454, Part of this research was performed at the Jet Propulsion Laboratory, California Institute of Technology, under contract with the National Aeronautics and Space Administration.

## REFERENCES

1. L. S. Rothman, R. R. Gamache, A. Goldman, J.-M. Flaud, R. H. Tipping, C. P. Rinsland, M. A. H. Smith, R. A. Toth, L. R. Brown, V. M. Devi, and D. C. Benner, "The HITRAN Database: 1992 Edition," *JQSRT* 48, 469 (1992).
2. D. Gautier and T. Owen, "The composition of outer planet atmospheres". In "Origin and Evolution of Planetary and Satellite Atmospheres", eds. S. K. Atreya, J. B. Pollack, and M. S. Matthews, Univ. Arizona Press, Tucson, pp. 487 (1989).
3. J. B. Pollack and P. Bodenheimer, "Theories of the origin and evolution of the giant planets", In "Origin and Evolution of Planetary and Satellite Atmospheres", eds. S. K. Atreya, J. B. Pollack, and M. S. Matthews, Univ. Arizona Press, Tucson, pp. 564 (1989).
4. L. A. Sromovsky, F. A. Best, H. E. Revercomb, and J. Hayden, *Space Sci. Rev.* 60, 233 (1992).
5. M. A. H. Smith and L. L. Gordley, *JQSRT* 29, 413 (1983).
6. B. Kivel, H. E. Fleming and W. G. Planet, *JQSRT* 17, 181 (1977).
7. W. J. Chu, E. W. Chiou, J. C. Larsen, L. W. Thomason, D. Rind, J. J. Buglia, S. Oltmans, M. P. McCormick, and L. M. McMaster, *J. Geophys. Res.* 98, 4857 (1993).
8. H. J. Liebe and T. A. Dillon, *J. Chem. Phys.* 50, 727 (1969).
9. T. Kasuga, H. Kuze, and 'I'. Shimizu, *J. Chem. Phys.* 69, 5195 (1978).
10. J. M. Dutta, C. R. Jones, T. M. Goyette, and F. C. DeLucia, *ICARUS* 102, 232 (1993).
11. S. Langlois, T. P. Birbeck, and R. K. Hanson, *J. Mol. Spectrosc.* 167, 272 (1994).

12. L. R. Brown and C. Plymate, in press, *JQSRT* 1996.
13. J. R. Izatt, H. Sakai, and W. S. Benedict, *J. Opt. Soc. Am. S9*, 19 (1969).
14. M. Godon, and A. Bauer, *Chem. Phys. Lett.* **147**, 189 (1988).
15. T. M. Goyette, and F. C. De Lucia, *J. Mol. Spectrosc.* **143**, 346 (1990).
16. J. R. Izatt, H. Sakai, and W. S. Benedict, *J. Opt. Soc. Am. S9*, 19 (1969).
17. D. Robert and J. Bonamy, *J. Phys. (Paris)* 40, 923 (1979).
18. R. Lynch, R. R. Gamache, and S. P. Neshyba, "Fully Complex implementation of the Robert-Bonamy Formalism: Half widths and Line Shifts of H<sub>2</sub>O Broadened by N<sub>2</sub>," submitted to *J. Chem. Phys.* November, 1995.
19. J.-M. Flaud and C. Camy-Peyret, private communications, (1990).
20. R. R. Gamache, J.-M. Hartmann, and L. Rosenmann, *JQSRT* S2, 481 (1994).
21. B. Labani, J. Bonamy, D. Robert, J. M. Hartmann and J. Taine, *J. Chem. Phys.* 84, 4256 (1986).
22. J. M. Hartmann, J. Taine, J. Bonamy, B. Labani and D. Robert, *J. Chem. Phys.* 86, 144 (1987).
- 23.** B. Labani, J. Bonamy, D. Robert, and J. M. Hartmann, *J. Chem. Phys.* 87, 2781 (1987).
24. S. P. Neshyba, and R. R. Gamache, *JQSRT* S0, 443 (1993).
25. S. Bouazza, A. Barbe, J. J. Plateaux, L. Rosenmann, J.-M. Hartmann, C. Camy-Peyret, J.-M. Flaud, and R. R. Gamache, *J. Mol. Spectrosc.* **157**, 271 (1993).
26. U. Fano and G. Racah, *irreducible Tensorial Sets*, Academic Press, Inc., New York (1959).
27. C. G. Gray and K. E. Gubbins, *Theory of Molecular Fluids*, vol. 1, Clarendon Press, Oxford (1984).

28. J. O. Hirschfelder, C. F. Curtiss, and R. B. Bird, *Molecular Theory of Gases and Liquids*, John Wiley and Sons, Inc., New York (1954).
29. H. C. Allen, Jr. and P. C. Cross, "*Molecular Vib-Rotors: The Theory and Interpretation of High Resolution Infrared Spectra*," J. Wiley, NY, (1963).
30. S. L. Shostak and J. S. Muentzer, *J. Chem. Phys.* 94, 5883 (1991).
31. J. Verhoeven and A. Dymanus, *J. Chem. Phys.* 52, 3222 (1970).
32. J. D. Poll and L. Wolniewicz, *J. Chem. Phys.* 68, 3053 (1978).
33. R. A. Sack, *J. Math. Phys.* 5, 260 (1964).
34. J. Downs, C. G. Gray, K. E. Gubbins, and S. Murad, *Mol. Phys* 37, 129 (1979).
35. S. P. Neshyba, R. Lynch, R. R. Gamache, T. Gabard and J.-P. Champion, *J. Chem. Phys.* **101**, 9412 (1994).
36. P. W. Anderson, *Phys. Rev.* 76, 647 (1949); 80, 511 (1950).
37. C. J. Tsao and B. Curnutte, Jr., *JQSRT*, 41 (1962).
38. R. Kubo, *J. Math. Phys.* 4, 174 (1963).
39. R. Lynch, *Ph.D. dissertation*, Physics Department, University of Massachusetts Lowell, June, 1995.
40. J.-P. Bouanich, *JQSRT*, 47243 (1992).
41. R. R. Gamache, *J. Mol. Spectrosc.* **114**, 31 (1985); R. R. Gamache and I. S. Rothman, *J. Mol. Spectrosc.* **128**, 360 (1988).
42. D. Crisp, D. A. Allen, D. H. Grinspoon, and J. B. Pollack, *Science* 253, 1263 (1991).
43. J. B. Pollack, J. B. Dalton, D. Grinspoon, R. B. Wattson, R. Freedman, D. Crisp, D. A. Allen, B. Bezard, C. DeBergh, L. P. Giver, Q. Ma, and R. Tipping, *ICARUS* **103**, 1 (1993).

44. R. R. Gamache, S. P Neshyba, J. J. Plateaux, A. Barbe, L Régalia, and J. B. Pollack, *J. Mol. Spectrosc.* 170, 131(1 995).
45. R. R. Gamache, unpublished results, (1 994).

## LIST OF TABLES

- TABLE I. Electrostatic moments for  $\text{H}_2\text{O}$  and  $\text{H}_2$
- TABLE II. Atom-atom Lennard-Jones (6-12) parameters
- TABLE III. Calculated Half-Widths for  $\text{H}_2\text{O}$  Broadened by  $\text{H}_2$  at 296 K and the measured values from Ref. 12.
- TABLE IV. Measured Halfwidths from Refs. 8-10 Compared with the Calculated Values.
- TABLE V. Calculated and Experimental Temperature Exponents for  $\text{H}_2\text{O}$  Broadened by  $\text{H}_2$
- Table VI, Measured Half widths of  $\text{H}_2\text{O}$  broadening by He and Temperature Dependence
- Table VII.  $\text{H}_2\text{O}$  broadening by He,  $\text{N}_2$ ,  $\text{O}_2$ ,  $\text{CO}_2$ , and  $\text{H}_2$  and the Ratio to the He-Broadened Value

TABLE I. Electrostatic moments for H<sub>2</sub>O, H<sub>2</sub>

Molecule	Multipole	Reference
H <sub>2</sub> O	$\mu=1.8549$ (9) $\times 10^{-18}$ esu	30
	$\Phi_{xx}=-0.13$ (3) $\times 10^{-26}$ esu	<b>31</b>
	$\Phi_{yy}=-2.50$ (2) $\times 10^{-26}$ esu	31
	$\Phi_{zz}=2.63$ (2) $\times 10^{-26}$ esu	31
H <sub>2</sub>	$\Theta_{zz}=-0.616$ (3) $\times 10^{-26}$ esu	32

TABLE II. Atom-atom Lennard-Jones (6-12) parameters

Pair	$\epsilon/K$	$\sigma/\text{Angstrom}$
H-N	20.5	3.0
C-N	34.3	3.45
Isotropic	119.3	3.838

TABLE 111. Calculated Half-Widths for 1120 Broadened by H<sub>2</sub> at 296 K and the measured values from Ref. 12.

l'	Ka'	Kc'	" Ka"	Kc"	(Cal)†	γ <sub>Exp</sub> [000]†	Δ C)/E % [000]	γ <sub>Exp</sub> [010]†	Δ C)/E % #!.QJ-
1	1	1	)	0	0	1.096		0.089 (1.0)	
1	1	0	1	0	1	.089		0.089 (1.4)	0.21
2	1	2	1	0	1	.089	.0854 (0.8)	0.0928 (3.4)	3.69
2	2	1	1	1	0	.080	.0847 (3.7)	0.0828 (0.8)	3.92
2	0	2	1	1	1	.092		0.0885 (0.6)	-4.39
2	2	0	1	1	1	.085			
2	1	1	2	0	2	.090		0.0878 (0.7)	-2.87
3	1	3	2	0	2	.082	.0785 (1.8)	0.0776 (0.6)	-5.52
3	3	1	2	0	2	.087			
2	2	0	2	1	1	.083		0.0832 (1.0)	-0.08
3	2	2	2	1	1	.082	.0829 (1.8)	0.0812 (0.3)	-0.80
2	2	1	2	1	2	.087	.0859 (1.7)	0.0878 (0.8)	1.44
3	0	3	2	1	2	.083	.0789 (1.1)	0.0761 (1.3)	-9.11
3	2	1	2	1	2	.086	.0899 (3.6)	0.0872 (2.7)	1.65
3	1	3	2	2	0	.087			
3	3	1	2	2	0	0.064	.0668 (5.4)	0.0623 (0.7)	-2.80
3	1	2	2	2	1	0.083		0.0826 (1.0)	-0.77
3	3	0	2	2	1	0.065	0.0663 (3.7)	0.0644 (1.4)	-0.80
3	1	2	3	0	3	0.085		0.0842 (1.9)	-0.96
3	3	0	3	0	3	0.084			
4	0	4	3	0	3	0.074			
4	1	4	3	0	3	0.073		0.0699 (2.2)	-4.13
4	3	2	3	0	3	0.080			
3	2	1	3	1	2	0.083		0.0805 (1.1)	-2.82
4	2	3	3	1	2	0.077	0.0803 (5.6)	0.0762 (0.7)	-1.51
4	4	1	3	1	2	0.077			
3	2	2	3	1	3	0.080	0.0766 (1.5)	0.0771 (1.1)	-3.24
4	0	4	3	1	3	0.072		0.0657 (1.0)	-10.32
4	2	2	3	1	3	0.081	0.0817 (1.1)	0.0808 (0.9)	-0.35
4	4	0	3	1	3	0.082			
3	3	0	3	2	1	0.071	0.0701 (3.5)	0.0697 (0.5)	-2.35
4	1	4	3	2	1	0.079		0.0799 (2.2)	0.58
4	3	2	3	2	1	0.071	0.0700 (2.6)	0.0679 (2.5)	-5.27
3	3	1	3	2	2	0.071		0.0683 (1.0)	-3.49
4	1	3	3	2	2	0.078		0.0731 (4.1)	-6.69
4	3	1	3	2	2	0.071		0.0652 (1.0)	-9.16
4	2	3	3	3	0	0.071		0.0689 (2.6)	-3.24
4	4	1	3	3	0	0.051	0.0517 (5.3)	0.0491 (3.1)	-4.02
4	0	4	3	3	1	0.081			
4	2	2	3	3	1	0.073		0.0731 (3.9)	0.22
4	4	0	3	3	1	0.051	0.0500 (2.4)	0.0484 (2.0)	-5.41
4	1	3	4	0	4	0.077		0.0699 (2.1)	-10.07
4	3	1	4	0	4	0.077			
5	1	5	4	0	4	0.063	0.0590 (4.7)	0.0570 (0.7)	-9.85
5	3	3	4	0	4	0.071	0.0785 (4.8)		
4	2	2	4	1	3	0.080		0.0758 (0.8)	-5.14
4	4	0	4	1	3	0.075			

5	2	4	4	1	3	.071	1.0698 (3.2)	-1.72	0.0687 (0.7)	-3.35
5	4	2	4	1	3	.073				
4	2	3	4	1	4	.070	1.0666 (0.6)	-5.47	0.0644 (0.9)	-9.16
4	4	1	4	1	4	.079				
5	0	5	\$	1	4	.062			0.0572 (2.0)	-8.04
5	2	3	4	1	4	.076	.0771 (1.5)	1.95	0.0769 (1.5)	1.70
5	4	1	'	\$	1	.074				
4	3	1	4	2	2	.073	.0696 (1.9)	-4.91	0.0692 (0.9)	-5.52
5	1	5	4	2	2	.074			0.0739 (5.5)	-0.09
5	3	3	4	2	2	.070	.0693 (1.9)	-1.40	0.0668 (1.4)	-5.27
4	3	2	4	2	3	.068	.0640 (1.5)	-6.59	0.0632 (1.0)	-8.03
5	1	4	4	2	3	3.070			0.0671 (0.9)	-4.93
5	3	2	4	2	3	.069			0.0639 (0.9)	-7.72
4	4	0	4	3	1	.060	.0556 (2.9)	-8.20	0.0576 (1.5)	-4.45
5	2	4	4	3	1	.068			0.0645 (3.7)	-4.72
5	4	2	4	3	1	.061			0.0541 (1.6)	-12.61
4	4	1	4	3	2	.059	.0562 (2.4)	-5.64	0.0558 (1.9)	-6.49
5	0	5	4	3	2	.072				
5	2	3	4	3	2	D.072			0.0680 (2,2)	-5.42
5	4	1	4	3	2	0.060			0.0540 (1.3)	-11.36
5	3	3	4	4	0	0.061				
5	5	1	4	4	0	0.044			0.0431 (1.2)	-2.02
5	1	4	4	4	1	0.073				
5	3	2	4	4	1	0.063			0.0608 (3.9)	-4.37
5	5	0	4	4	1	0.044			0.0425 (1.8)	-3.42
5	1	4	5	0	5	0.068	.0665 (2.4)	-1.70	0.064 (1.0)	-5.76
5	3	2	5	0	5	0.070				
6	1	6	5	0	5	0.053	.0502 (3.5)	-5.83	0.0498 (1.8)	-6.78
6	3	4	5	0	5	0.063	.0631 (2.0)	-0.02	0.0622 (3.2)	-1.46
5	2	3	5	1	4	0.075			0.0719 (0.7)	-4.36
5	4	1	5	1	4	0.070				
6	2	5	5	1	4	0.064			0.0618 (0.5)	-3.61
6	4	3	5	1	4	0.067				
5	2	4	5	1	5	0.061	.0572 (3.2)	-7.46	0.0580 (0.7)	-5.98
5	4	2	5	1	5	0.070				
6	0	6	5	1	5	0.053			0.0475 (0.7)	-10.54
6	2	4	5	1	5	0.070			0.0683 (2.7)	-2.08
6	4	2	5	1	5	0.067				
5	3	2	5	2	3	0.072	.0689 (1.2)	-5.17	0.0674 (1.6)	-7.51
6	1	6	5	2	3	0.070				
6	3	4	5	2	3	0.068	.0700 (5.6)	2.94	0.0623 (2,4)	-9.14
6	5	2	5	2	3	0.068				
5	3	3	5	2	4	0.063	.0567 (2.0)	-10.72	0.0582 (3.0)	-7.96
6	1	5	5	2	4	0.062	.0596 (3.0)	-4.19	0.0580 (1.0)	-7.15
6	3	3	5	2	4	0.068			0.0622 (2.5)	-6.38
5	4	1	5	3	2	0.06:	.0575 (2.5)	-9.39	0.0564 (1.3)	-11.52
6	2	5	5	3	2	0.064			0.0580 (5.7)	-10.98
6	4	3	5	3	2	0.062			0.0569 (2.4)	-8.80
5	4	2	5	3	3	0.060	.0539 (1.5)	-11.57	0.0530 (3.2)	-13.46
6	0	6	5	3	3	0.064				
6	2	4	5	3	3	0.068			0.0647 (5.6)	-5.07
6	4	2	5	3	3	0.06[			0.0540 (2.7)	-10.88
5	5	0	5	4	1	0.053	.0491 (2.7)	-7.64	0.0519 (2.5)	-1.84

6	3	4	5	4	1	0.060			0.0543 (2.3)	-10.78
6	5	2	5	4	1	0.054			0.0487 (2.1)	-10.96
5	5	1	5	4	2	0.053			0.0498 (4.0)	-5.85
6	1	5	5	4	2	0.066				
6	3	3	5	4	2	0.064				
6	5	1	5	4	2	0.054			0.0486 (2.7)	-10.88
6	4	3	5	5	0	0.056				
6	6	1	5	5	0	0.042				
6	4	2	5	5	1	0.057				
6	6	0	5	5	1	0.042				
6	1	5	6	0	6	0.058	0.0571 (2.8)	-2.42	0.0571 (1 .8)	-2.50
6	3	3	6	0	6	0.067				
7	1	7	6	0	6	0.046			0.0423 (0.5)	-7.92
7	3	5	6	0	6	0.057				
6	2	4	6	1	5	0.069			0.0655 (0.9)	-5.59
6	4	2	6	1	5	0.064				
7	2	6	6	1	5	0.056	0.0551 (2.1)	-2.50	0.0536 (3,0)	-5.46
7	4	4	6	1	5	0.061				
6	2	5	6	1	6	0.054	0.0530 (1 .7)	-2.47	0.0513 (0.7)	-5.97
6	4	3	6	1	6	0.064				
7	0	7	6	1	6	0.045			0.0422 (0.9)	-7.49
7	2	5	6	1	6	0.063			0.0650 (3.3)	2.49
7	4	3	6	1	6	0.063				
6	3	3	6	2	4	0.071			0.0666 (3.2)	-7.03
7	1	7	6	2	4	0.065				
7	3	5	6	2	4	0.065			0.0614 (4.1)	-5.23
7	5	3	6	2	4	0.066				
6	3	4	6	2	5	0.058	0.0551 (0.9)	-5.11	0.0531 (1.1)	-9.07
7	1	6	6	2	5	0.055			0.0509 (0.9)	-7.26
7	3	4	6	2	5	0.064	0.0650 (1 .2)	1.69	0.0627 (3.2)	-1.91
7	5	2	6	2	5	0.061				
6	4	2	6	3	3	0.064			0,0595 (2.4)	-6.97
7	2	6	6	3	3	0.062				
7	4	4	6	3	3	0.062			0.0599 (3.6)	-3.43
6	4	3	6	3	4	0.058	0.0551 (3.2)	-5.25	0.0529 (1 .7)	-9.73
7	0	7	6	3	4	0.057				
7	2	5	6	3	4	0.063	0.0631 (1.9)	-0.38	0.0613 (2.4)	-3.32
7	4	3	6	3	4	0.059	0.0564 (2.6)	-4.23	0.0554 (2.6)	-6.10
6	5	1	6	4	2	0.056			0.0480 (4.5)	-17.05
7	3	5	6	4	2	0.058				
7	5	3	6	4	2	0.056	0.0532 (4.6)	-4.72	0.0509 (2.5)	-9.56
6	5	2	6	4	3	0.055			0.0480 (3.0)	-15.54
7	1	6	6	4	3	0.060				
7	3	4	6	4	3	0.063			0.0602 (4.3)	-5.27
7	5	2	6	4	3	0.055	0.0524 (3.2)	-5,17	0.0513 (2.9)	-7.53
6	6	0	6	5	1	0.050			0.0411 (2.5)	-22.03
7	4	4	6	5	1	0.056				
7	6	2	6	5	1	0.051	0.0482 (2.6)	-5.81	0.0491 (3.2)	-3.87
6	6	1	6	5	2	0,050				
7	4	3	6	5	2	0,058				
7	6	1	6	5	2	0.051	0.0489 (2.5)	-4.27	0.0481 (2.3)	-6.00
7	5	3	6	6	0	0,054				
7	7	1	6	6	0	0,041				
7	5	2	6	6	1	0.054				

7	7	0	6	6	1	0.041			0.0427 (3.9)	3.90
7	1	6	7	0	7	0.050			0.0495 (1.1)	-1.98
7	3	4	7	0	7	0.064				
8	1	8	7	0	7	0.040			0.0387 (1 .0)	-3.68
8	3	6	7	0	7	0.051				
7	2	5	7	1	6	0.062			0.0604 (0.8)	-3.02
7	4	3	7	1	6	0.060				
8	2	7	7	1	6	0.049	0.0499 (5.7)	1.43	0.0476 (1 .2)	-3.44
8	4	5	7	1	6	0.055				
7	2	6	7	1	7	0.048	0.0481 (1 .7)	-0.25	0.0458 (1 .5)	-5.28
8	0	8	7	1	7	0.040			0.0380 (1 .2)	-5.26
8	2	6	7	1	7	0.057				
7	3	4	7	2	5	0.069			0.0669 (1 .4)	-2.75
7	5	2	7	2	5	0.064				
8	1	8	7	2	5	0.060				
8	3	6	7	2	5	0.060	0.0609 (0.9)	2.00	0.0599 (2.2)	0.37
8	5	4	7	2	5	0.062				
7	3	5	7	2	6	0.053	0.0511 (2.8)	-4.17	0.0500 (2.9)	-6.57
8	1	7	7	2	6	0.048	0.0466 (1 .3)	-2.93	0.0450 (2.7)	-6.71
8	3	5	7	2	6	0.061				
7	4	3	7	3	4	0.064	0.0631 (3.1)	-1.67	0.0619 (1.2)	-3.64
8	2	7	7	3	4	0.060				
8	4	5	7	3	4	0.061	0.0636 (2.9)	3.86	0.0613 (3.6)	0.17
7	4	4	7	3	5	0.055			0.0515 (4.0)	-7.28
8	0	8	7	3	5	0.052				
8	2	6	7	3	5	0.058	0.0597 (4 .3)	2.87	0.0556 (3.0)	-4.29
8	4	4	7	3	5	0.058	0.0590 (3.0)	1.90	0.0562 (4.5)	-2.99
7	5	2	7	4	3	0.057	0.0551 (1 .6)	-3.41	0.0518 (5.4)	-10.00
8	3	6	7	4	3	0.056				
8	5	4	7	4	3	0.056	0.0571 (2.2)	2.12	0.0544 (3.5)	-2.84
7	5	3	7	4	4	0.055			0.0480 (2.7)	-14.22
8	1	7	7	4	4	0.055				
8	3	5	7	4	4	0.061				
8	5	3	7	4	4	0.054	0.0558 (2.7)	2.76	0.0515 (4.9)	-5.36
7	6	1	7	5	2	0.053			0.0514 (1.8)	-3.73
8	4	5	7	5	2	0.055			0.0542 (3.5)	-1.12
8	6	3	7	5	2	0.052			0.0502 (4.5)	-4.59
7	6	2	7	5	3	0.053			0.0478 (4.1)	-11.10
8	4	4	7	5	3	0.058				
8	6	2	7	5	3	0.052			0.0547 (2.3)	4.37
7	7	0	7	6	1	0.048				
8	5	4	7	6	1	0.054				
8	7	2	7	6	1	0.048				
7	7	1	7	6	2	0.048				
8	5	3	7	6	2	0.055				
8	7	1	7	6	2	0.048				
8	6	3	7	7	0	0.051				
8	8	1	7	7	0	0.039				
8	8	0	7	7	1	0.039				
8	1	7	8	0	8	0.044			0.0438 (4.9)	-0.62
8	3	5	8	0	8	0.061				
9	1	9	8	0	8	0.036			0.0346 (5.0)	-3.89
9	3	7	8	0	8	0.046				
8	2	6	8	1	7	0.055			0.0532 (3.4)	-3.72

8	4	4	8	1	7	0.057				
9	2	8	8	1	7	0.043			0.0434 (3.5)	-0.03
9	4	6	8	1	7	0.050				
8	2	7	8	1	8	0.043	0.0427 (2.9)	-0.95	0.0426 (2.0)	-1.18
9	0	9	8	1	8	0.036			0.0344 (3.6)	-4.44
9	2	7	8	1	8	0.050				
8	3	5	8	2	6	0.065			0.0629 (5.3)	-2.72
8	5	3	8	2	6	0.059				
9	1	9	8	2	6	0.054				
9	3	7	8	2	6	0.054				
9	5	5	8	2	6	0.057				
8	3	6	8	2	7	0.048	0.0491 (1 .9)	1.34	0.0476 (2.1)	-1.87
9	1	8	8	2	7	0.043	0.0432 (3.6)	0.95	0.0422 (1 .3)	-1.52
9	3	6	8	2	7	0.058				
8	4	4	8	3	5	0.064				
9	2	8	8	3	5	0.058				
9	4	6	8	3	5	0.059				
8	4	5	8	3	6	0.052			0.0513 (3.7)	-1.48
9	0	9	8	3	6	0.048				
9	2	7	8	3	6	0.052			0.0536 (3.6)	3.14
9	4	5	8	3	6	0.057			0.0558 (4.4)	-1.82
8	5	3	8	4	4	0.057				
9	3	7	8	4	4	0.055				
9	5	5	8	4	4	0.056				
8	5	4	8	4	5	0.053			0.0532 (5.4)	0.12
9	1	8	8	4	5	0.051				
9	3	6	8	4	5	0.059			0.0644 (5.0)	8.30
9	5	4	8	4	5	0.053			0.0543 (1 .7)	2.58
8	6	2	8	5	3	0.053				
9	4	6	8	5	3	0.053				
9	6	4	8	5	3	0.052				
8	6	3	8	5	4	0.053			0.0494 (4.8)	-6.34
9	4	5	8	5	4	0.058				
9	6	3	8	5	4	0.051				
8	7	1	8	6	2	0.050				
9	5	5	8	6	2	0.053				
9	7	3	8	6	2	0.049				
8	7	2	8	6	3	0.050				
9	5	4	8	6	3	0.053				
9	7	2	8	6	3	0.049				
8	8	0	8	7	1	0.044				
9	8	2	8	7	1	0.044				
8	8	1	8	7	2	0.044				
9	6	3	8	7	2	0.051				
9	8	1	8	7	2	0.044				
9	9	0	8	8	1	0.035				
9	1	8	9	0	9	0.040			0.0413 (1 .9)	4.34
10	1	10	9	0	9	0.033			0.0341 (1.2)	3.27
1	0	3	8	9	0	9	0.043			
9	2	7	9	1	8	0.049			0.0497 (2.7)	2.17
9	4	5	9	1	8	0.056				
10	2	9	9	1	8	0.039			0.0419 (1 .6)	5.99
1	0	4	7	9	1	8	0.047			
9	2	8	9	1	9	0.039			0.0383 (3.6)	-2.31

10	0	10	9	1	9	0.033	0.0342 (2.5)	3.57	
1	0	2	8	9	1	9	0.045		
9	3	6	9	2	7	0.060	0.0603 (5.3)	0.73	
9	5	4	9	2	7	0.055			
10	1	10	9	2	7	0.048			
1	0	3	8	9	2	7	0.049	0.0520 (4.6)	6.28
1	0	5	6	9	2	7	0.053		
9	3	7	9	2	8	0.044	0.0464 (5.7)	4.24	
10	1	9	9	2	8	0.039	0.0412 (5.0)	4.91	
1	0	3	7	9	2	8	0.054		
9	4	5	9	3	6	0.063	0.0614 (4.5)	-2.43	
10	2	9	9	3	6	0.056			
1	0	4	7	9	3	6	0.057		
9	4	6	9	3	7	0.049			
1	0	2	8	9	3	7	0.047		
10	4	6	9	3	7	0.056			
9	5	4	9	4	5	0.057			
10	3	8	9	4	5	0.054			
1	0	5	6	9	4	5	0.056		
9	5	5	9	4	6	0.051			
1	0	3	7	9	4	6	0.056		
10	5	5	9	4	6	0.052			
9	6	3	9	5	4	0.052			
1	0	4	7	9	5	4	0.051		
1	0	6	5	9	5	4	0.051		
9	6	4	9	5	5	0.051			
1	0	4	6	9	5	5	0.057		
10	6	4	9	5	5	0.050			
9	7	2	9	6	3	0.049			
10	5	6	9	6	3	0.051			
1	0	7	4	9	6	3	0.048		
9	7	3	9	6	4	0.049			
1	0	5	5	9	6	4	0.053		
1	0	7	3	9	6	4	0.048		
9	8	1	9	7	2	0.046			
1	0	6	5	9	7	2	0.050		
1	0	8	3	9	7	2	0.046		
9	8	2	9	7	3	0.046			
10	1	9	10	0	10	0.037	0.0408 (5.1)	10.54	
11	1	11	10	0	10	0.031			
1	0	2	8	10	1	9	0.044	0.0459 (3,4)	4.40
11	2	10	10	1	9	0.037			
1	0	2	9	10	1	10	0.036	0.0376 (4.5)	3.22
11	0	11	10	1	10	0.031			
11	2	9	10	1	10	0.042			
1	0	3	7	1	0	2	8	0.055	
11	3	9	10	2	8	0.045			
1	0	3	8	10	2	9	0.042		
11	1	10	10	2	9	0.037	0.0414 (2.3)	10.81	
1	1	3	8	10	2	9	0.050		
1	0	4	6	10	3	7	0.061		
11	4	8	10	3	7	0.054			
1	0	4	7	10	3	8	0.046		
11	2	9	10	3	8	0.044			

11	4	7	10	3	8	0.054		
1	0	5	5	1	0	4	6	0.058
11	3	9	1	0	4	6	0.055	
11	5	7	1	0	4	6	0.056	
10	5	6	1	0	4	7	0.049	
11	3	8	1	0	4	7	0.052	
11	5	6	10	4	7	0.052		
1	0	6	4	1	0	5	5	0.052
11	4	8	1	0	5	5	0.051	
11	6	6	1	0	5	5	0.051	
10	6	5	1	0	5	6	0.049	
1	1	4	7	1	0	5	6	0.056
11	6	5	1	0	5	6	0.049	
1	0	7	3	1	0	6	4	0.048
10	7	4	10	6	5	0.048		
11	5	6	1	0	6	5	0.052	
11	7	4	1	0	6	5	0.047	
10	8	3	1	0	7	4	0.046	
11	1	10	11	0	11	0.035		
12	1	12	11	0	11	0.030		
11	2	9	11	1	10	0.041		
12	2	11	11	1	10	0.036		
11	2	10	11	1	11	0.035		
12	0	12	11	1	11	0.030		
11	3	8	11	2	9	0.051		
12	3	10	11	2	9	0.043		
11	3	9	11	2	10	0.040		
12	1	11	11	2	10	0.036		
11	4	7	11	3	8	0.059		
1	2	4	9	11	3	8	0.051	
11	4	8	11	3	9	0.045		
12	2	10	11	3	9	0.042		
11	5	6	11	4	7	0.058		
1	2	5	8	11	4	7	0.055	
11	5	7	11	4	8	0.048		
1	2	3	9	11	4	8	0.049	
11	6	5	11	5	6	0.051		
12	4	9	11	5	6	0.051		
1	2	6	7	11	5	6	0.050	
11	6	6	11	5	7	0.048		
11	7	4	11	6	5	0.047		
12	1	11	12	0	12	0.034		
13	1	13	12	0	12	0.030		
12	2	10	12	1	11	0.040		
13	2	12	12	1	11	0.036		
12	2	11	12	1	12	0.034		
13	0	13	12	1	12	0.030		
12	3	9	12	2	10	0.047		
13	3	11	12	2	10	0.042		
12	3	10	12	2	11	0.040		
13	1	12	12	2	11	0.036		
12	4	8	1	2	3	9	0.055	
1	2	4	9	12	3	10	0.044	
13	2	11	12	3	10	0.042		

0.0341 (2.1) 12.32

0.0399 (5.0) 9.55

TABLE IV. Measured Half widths' from Refs. 8-10 Compared with the Calculated Values.

Transition	Temp.	Measured†	Ref.	Calculated	% Error
616←523	293 K	0.0710 ( $\pm$ 0.0076)	9	0.0687	3.2 _
616←523	300 K	0.0834 ( $\pm$ 0.0021)	8	0.0680	18.
313←220	300 K	0.0811 (*0.0020)	<b>10</b>	<b>0.0860</b>	<b>-6.0</b> _
414←321	300 K	0.0811 ( $\pm$ 0.0020)	10	0.0788	2.8

† in units of  $\text{cm}^{-1}/\text{atm}$ .

12	5	7	1	2	4	8	0.056			
12	5	8	1	2	4	9	0.047			
13	3	10	1	2	4	9	0.047			
12	6	7	1	2	5	8	0.047			
13	1	12	13	0	13		0.034			
13	2	11	13	1	12		0.040			
1	3	4	9	13	3	10	0.052			
1	3	5	8	1	3	4	9	0.054		
14	1	14	13	0	13		0.030			
14	2	13	13	1	12		0.037			
14	0	14	13	1	13		0.030			
14	3	12	13	2	11		0.042			
14	1	13	13	2	12		0.037			
15	1	15	14	0	14		0.031			
15	0	15	14	1	14		0.031			
15	1	14	14	2	13		0.038			

Table VI. Measured Halfwidths of H<sub>2</sub>O broadening by He and Temperature Dependence

Transition						$\gamma \dagger \times 10^3$	T /K	n	Ref.
3	1	3	2	2	0	21.7±0.2	300.	0.39±0.10	14
3	1	3	1	2	0	21.4±0.2	315.	<b>0.3930.10</b>	14
3	1	3	2	2	0	21.1±0.2	330.	<b>0.3930.10</b>	14
3	1	3	2	2	0	<b>0.430.2</b>	360.	<b>0.39*0.10</b>	14
3	1	3	2	2	0	10.1±0.2	375.	0.39±0.10	14
3	1	3	2	2	0	9.6±0.3	40.	0.39±0.10	14
4	1	4	3	2	1	10.3±0.2	40.	0.34±0.09	14
4	1	4	3	2	1	<b>19.830.2</b>	44.	0.34±0.09	14
4	1	4	3	2	1	19.3±0.2	48.	0.34±0.09	14
		4		2	1	18.9±0.2	73.	0.34±0.09	14
		6		2	3	24.6±0.5	90.		8
		6		2	3	20.0±1.3	93.		9
		3		2	0	18.0±1.8	97.	0.49±0.02	15
		3		2	0	20.3±2.0	44.	0.49±0.02	15
		3		2	0	22.0±2.2	97.	0.49±0.02	15
		3		2	0	4.1±2.4	64.	0.49±0.02	15
	1	3	2	2	0	9.4±2.9	92.	0.49±0.02	15
		3	2	2	0	2.2±3.2	77.	0.49±0.02	15
		3	2	2	0	4.2±3.4	62.	0.49±0.02	15
	1	3	2	2	0	<b>7.253.7</b>	44.	0.49±0.02	15
		3	2	2	0	8.2±3.8	20.	0.49±0.02	15
		3	2	2	0	10.5±4.0	104.	<b>0.4930.02</b>	15
		3	2	2	0	9.3±3.9	103.	0.49±0.02	15
		3	2	2	0	14.1±4.4	87.	0.49±0.02	15
		3	2	2	0	<b>6.9? 4.7</b>	83.	0.49±0.02	15
6	6	1	5	3	2	50.0±25.0	353.		16
6	6	0	5	3	3	<b>30.0±15.0</b>	353.		16
7	6	1	6	3	4	50.0±25.0	353.		16
7	6	2	6	3	3	30.0±15.0	353.		16
8	6	3	7	3	4	80.0±40.0	353.		16
12	5	8	11	2	9	40.0±20.0	353.		16
13	4	9	12	3	10	50.0±25.0	<b>3 5 3</b>		16

† in units of cm<sup>-1</sup>/atm

Table V, Calculated and Experimental Temperature Exponents for H<sub>2</sub>O  
Broadened by H<sub>2</sub>

J'	Ka'	Kc'	J''	Ka''	Kc''	n(Cal)	n(Exp)
1	0	1	0	0	0	0.718(0.038)	0.87(0.04)
2	2	1	1	1	0	0.575(0.020)	
2	2	0	2	1	1	0.610(0.007)	
2	1	1	2	1	2	0.644(0.036)	1.02(0,27)
2	2	0	3	1	2	0.606(0.008)	
2	2	0	3	1	3	0.590(0.052)	0.95(0.07)
4	1	4	3	2	1	0.543(0.051)	0.85(0.05)
3	1	2	3	2	1	0.609(0.013)	0.40(0,10)
3	2	1	3	2	2	0.533(0.056)	0.62(0.16)
3	3	0	3	3	1	0.361(0.053)	0.35(0,13)
3	3	1	3	3	0	0.361(0.053)	0.76(0.25)
4	1	3	4	2	2	0.584(0.027)	1.50(0.38)
5	3	2	4	2	3	0.441(0.083)	
4	3	2	4	3	1	0.414(0.084)	0.39(0.11)
4	3	1	4	3	2	0.414(0,084)	0.26(0.10)
6	1	6	5	2	3	0.485(0.021)	
6	1	6	5	0	5	0.264(0.125)	
6	2	5	5	1	4	0.413(0.049)	
6	2	4	5	1	5	0.478(0.042)	
6	3	4	5	2	3	0.473(0.027)	
5	1	4	5	2	3	0.545(0.030)	0.72(0.20)
6	3	3	5	2	4	0.430(0.055)	
5	3	3	5	3	2	0.407(0.075)	0,25(0.10)
6	4	3	5	3	2	0.394(0.056)	
6	4	2	5	3	3	0.349(0.088)	
6	5	2	5	4	1	0.327(0.048)	
6	5	1	5	4	2	0.324(0,049)	
6	6	1	5	5	0	0.304(0.101)	
6	6	0	5	5	1	0.304(0,101)	
7	5	3	6	4	2	0.351(0.027)	
8	6	3	7	5	2	0.378(0.127)	
9	7	3	8	6	2	0.374(0.196)	
10	8	3	9	7	2	0.311(0.148)	

Table VII. H<sub>2</sub>O broadening by He, N<sub>2</sub>, O<sub>2</sub>, CO<sub>2</sub>, and H<sub>2</sub> and the Ratio to the He-Broadened Value

#†	$\gamma(\text{He})^{\dagger\dagger}$	$\gamma(\text{N}_2)^{\dagger\dagger}$	Ratio	$\gamma(\text{O}_2)^{\dagger\dagger}$	Ratio	$\gamma(\text{CO}_2)^{\dagger\dagger}$	Ratio	$\gamma(\text{H}_2)^{\dagger\dagger}$	Ratio
1	0.0218	<b>0.105</b>	<b>0.21</b>	0.0696	0.31	<b>0.157</b>	<b>0.14</b>	0.0867	0.25
2	<b>0.0204</b>	<b>0.102</b>	<b>0.20</b>	0.0671	0.30	0.152	0.13	0.0794	0.26
3	<b>0.0248</b>	<b>0.0967</b>	<b>0.26</b>	0.0637	0.39	0.144	0.17	0.0695	0.36

† See text for transitions.

†† in units of cm<sup>-1</sup>/atm

## LIST OF FIGURES

- Figure 1      percent Difference, measurements of Ref. 12 minus calculated values versus Energy ordered Index for the pure rotation band (■) and the  $\nu_2$  band (x) .
- Figure 2       $\ln \{y(T) / y(I'o)\}$  versus  $\ln\{T/T_0\}$ , the slope of the line is the temperature exponent, shown are the maximum (1 01 ← 0 0 0) and the minimum (6 1 6 ← 5 0 5) calculated temperature exponents.
- Figure 3      Calculated (✱) and experimental (o) temperature exponents with corresponding error bars versus line number (see Table V).
- Figure 4      Calculated temperature exponents with error bars (see Table V) versus  $(K_a'' - K_c'')$  for transitions with  $J''=5$ .
- Figure 5      Percent difference calculated minus estimated halfwidth versus  $(J'' - I' J')/2$  for the average method (■) and the polynomial method (-t).

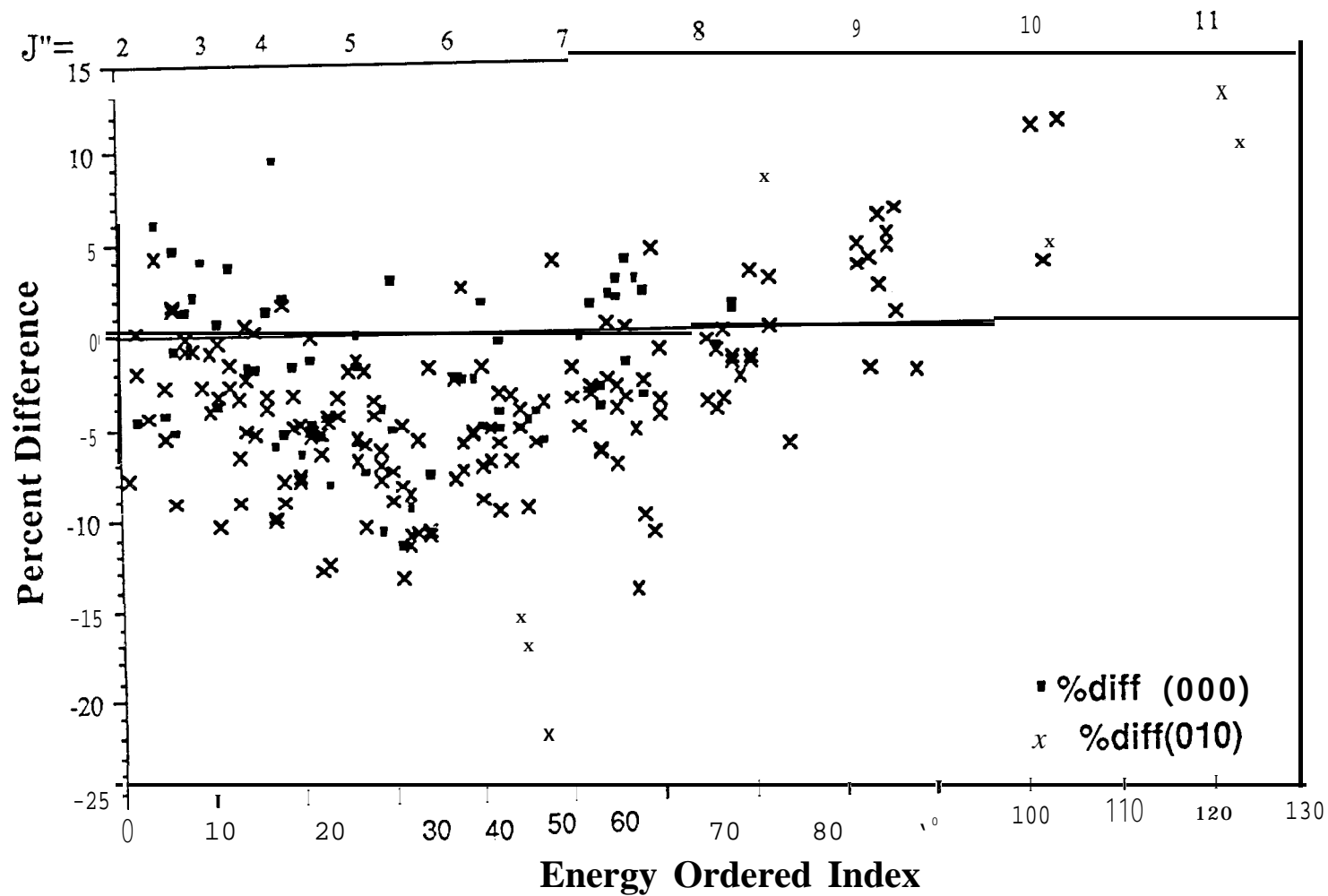


Figure 1 Percent Difference, measurements of Ref. 12 minus calculated values versus Energy ordered Index for the pure rotation band (■) and the  $\nu_2$  band (x).

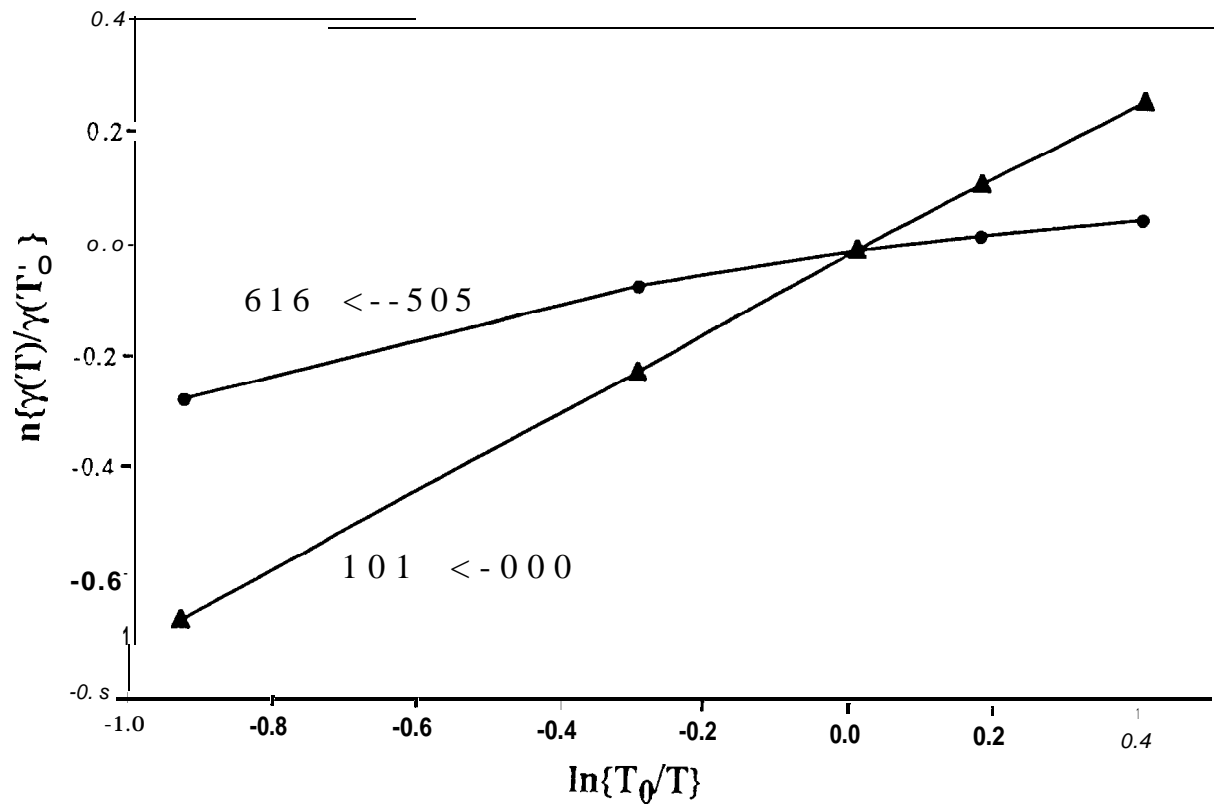


Figure 2  $\ln\{\gamma(T)/\gamma(T_0)\}$  versus  $\ln\{T/T_0\}$ , the slope of the line is the temperature exponent, shown are the maximum (1 0 1 ← 0 0 0) and the minimum (6 1 6 ← 5 0 5) calculated temperature exponents.

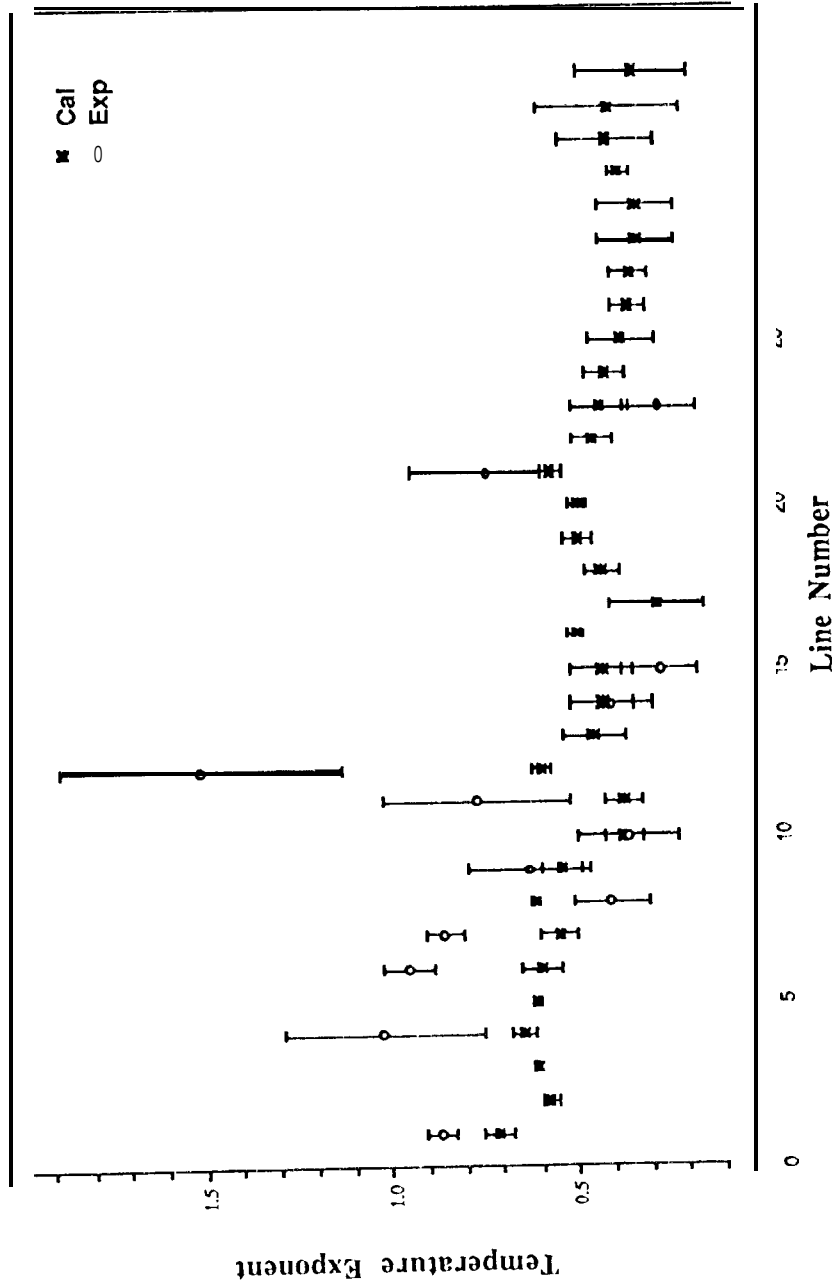


Figure 3 Calculated (\*) and experimental (o) temperature exponents with corresponding error bars versus line number (see Table V).

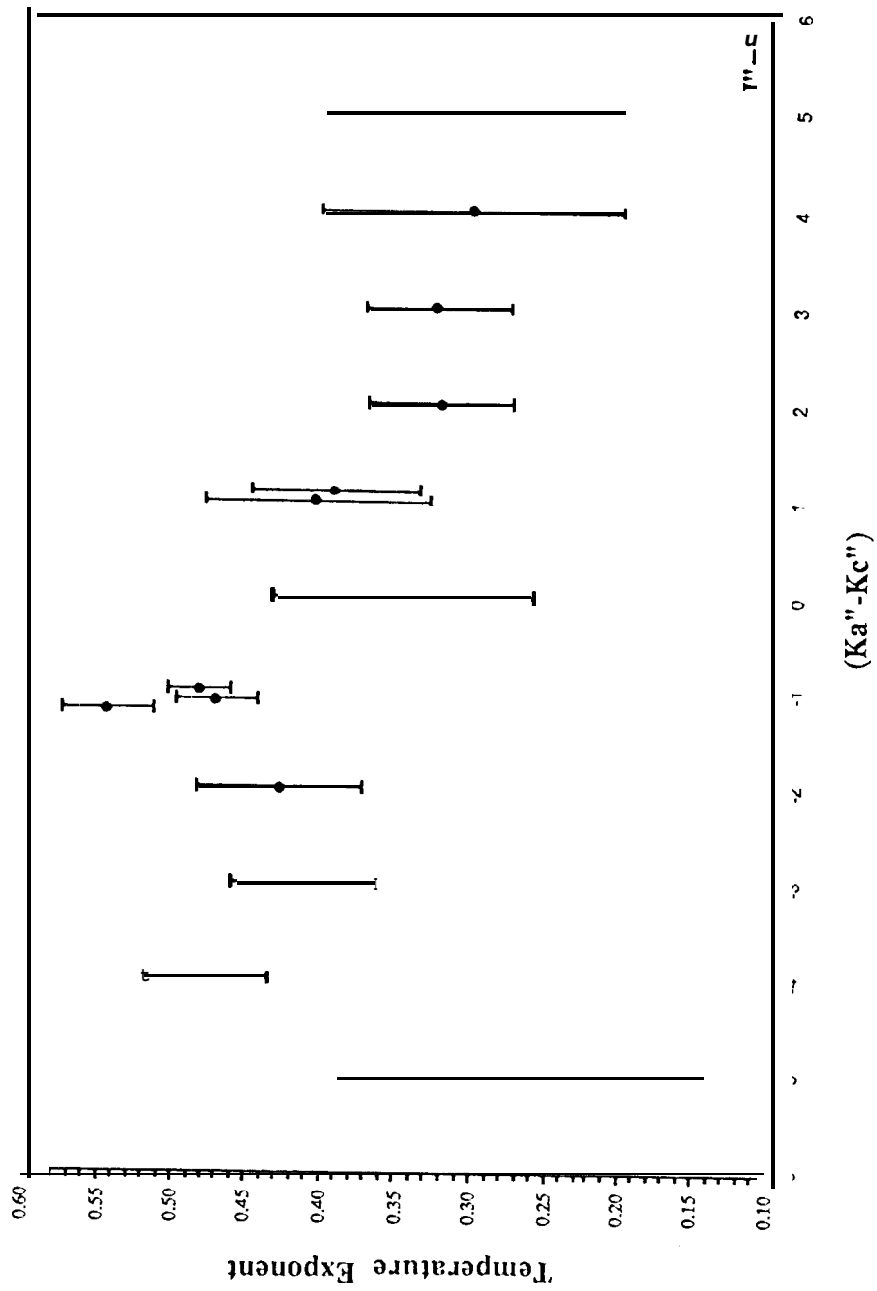


Figure 4 Calculated temperature exponents with error bars (see Table V) versus  $(K_a'' - K_c'')$  for transitions with  $J''=5$ .

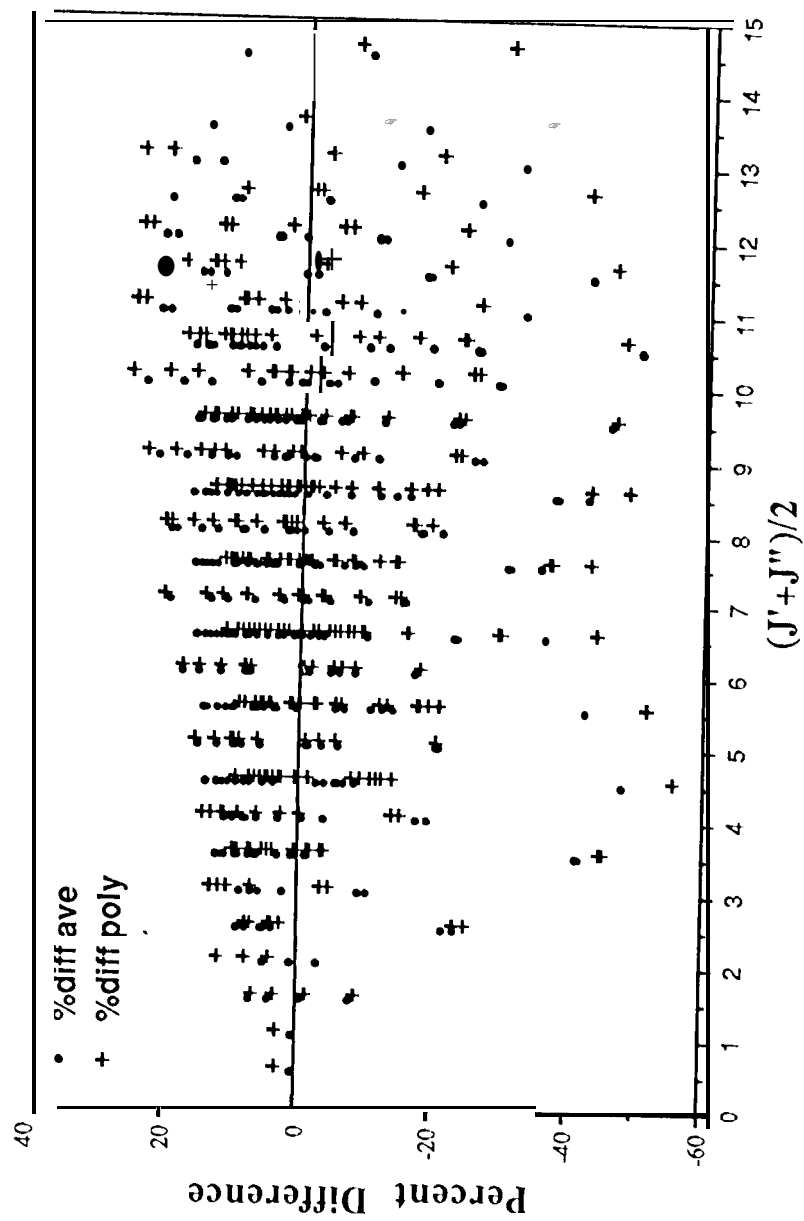


Figure 5 Percent difference calculated minus estimated halfwidth versus  $(J'+J'')/2$  for the average method (•) and the polynomial method (+).